Geosci. Model Dev., 16, 1875–1886, 2023
https://doi.org/10.5194/gmd-16-1875-2023

Geoscientific Model Development
Open Access
EGU

Assessing methods for representing soil heterogeneity through a flexible approach within the Joint UK Land Environment Simulator (JULES) at version 3.4.1

Heather S. Rumbold, Richard J. J. Gilham, and Martin J. Best

Met Office, Exeter, Devon, EX1 3PB, United Kingdom

Correspondence: Heather S. Rumbold (heather.rumbold@metoffice.gov.uk)

Received: 24 May 2022 – Discussion started: 5 August 2022
Revised: 2 November 2022 – Accepted: 12 December 2022 – Published: 4 April 2023

Abstract. The interactions between the land surface and the atmosphere can impact weather and climate through the exchanges of water, energy, carbon and momentum. The properties of the land surface are important when modelling these exchanges correctly especially with models being used at increasingly higher resolution. The Joint UK Land Environment Simulator (JULES) currently uses a tiled representation of land cover but can only model a single dominant soil type within a grid box. Hence, there is no representation of sub-grid-scale soil heterogeneity. This paper introduces and evaluates a new flexible surface–soil tiling scheme in JULES. Several different soil tiling approaches are presented for a synthetic case study. The changes to model performance have been compared to the current single-soil scheme and a high-resolution "Truth" scenario. Results have shown that the different soil tiling strategies do have an impact on the water and energy exchanges due to the way vegetation accesses the soil moisture. Tiling the soil according to the surface type, with the soil properties set to the dominant soil type under each surface is the best performing configuration. The results from this setup simulate water and energy fluxes that are the closest to the high-resolution Truth scenario but require much less information on the soil type than the high-resolution soil configuration.

1 Introduction

Land surface models (LSMs) are an important aspect of numerical weather prediction and climate simulations. They can be applied in both standalone and coupled mode and on grids covering a range of spatial and temporal scales from high-resolution weather forecasts (less than 1 km for several days) through to Earth System modelling for climate prediction (over 100 km for up to 100 years). Historically LSMs were considered to be a bottom boundary condition, the primary role being to provide fluxes of momentum, heat, moisture and carbon back to the atmospheric models. However, in the last couple of decades an understanding of the importance and impact of land surface processes on the overlying atmosphere has grown. A number of studies have shown that the spatial variability of land surface properties has a direct impact on the surface fluxes (Eltahir and Bras, 1996; Eltahir, 1998; Betts and Ball, 1998; Hohenegger et al., 2009) and therefore needs to be accounted for. The ability of LSMs to represent these properties at increasingly high resolution is limited by the resolution of the land ancillary information available (for example soil and vegetation types) and the computational expense of running at high resolution. Many land surface models have therefore adopted methods to represent sub-grid heterogeneity without the need for running at high resolution.

In general there are three main approaches currently used to represent sub-grid heterogeneity: mosaic, tiled and aggregated. The mosaic approach uses a sub-grid to represent every pixel of land for which data are available. Each pixel has an appropriate set of parameters describing the physical behaviour of the surface and soil (e.g. soil texture, vegetation fractions, albedo, leaf area index, roughness length). The tiling approach has the same parameter set but groups these pixels into a smaller number of distinct surface types each with representative parameter values. The aggregation approach attempts to represent the average properties of the

grid box surface as a single set of representative parameters. However, Heinemann and Kerschgens (2005) highlighted that the terminology of the different approaches used (tiled, aggregated, mosaic) is ambiguous in the literature, and this is compounded by the need for different formulations imposed by different modelling architectures. This results in no one best approach being clearly recommended by the literature.

The community land surface model JULES (Joint UK Land Environment Simulator) is the land component of the Met Office Unified Model (UM) (Walters et al., 2019). JULES calculates the exchanges of energy and momentum between the surface and the atmosphere by representing a range of surface and sub-surface processes, including snow, surface and soil hydrology, and vegetation physiology and dynamics. JULES currently uses a tiled model to represent surface heterogeneity with separate energy and water fluxes computed for each surface type within an atmospheric grid box (Essery et al., 2003). However, each of the surfaces in the tiled scheme currently experiences the same sub-surface soil conditions; i.e. there is a single soil column per grid box. Due to the non-linear nature of soil processes, the dominant soil type is used for each grid box (rather than an average soil type), and soil parameters associated with this soil type are then used. The consequence of using this current method is that some of the spatial soil heterogeneity is lost when regridding from the ancillary source grid to the model grid and through selecting the dominant soil on the model grid. Therefore, a soil tiling approach that can represent the sub-grid-scale soil heterogeneity should be beneficial. Table 1 gives examples of LSMs used by the land modelling community and the approaches used by them to model sub-grid soil heterogeneity. H-TESSEL uses a dominant soil texture class (i.e. course, medium, medium fine, fine, very fine, organic) for every grid box, whilst CLM and ISBA have a single soil with properties aggregated within each grid box (Noilhan and Mahfouf, 1999). Most other LSMs have adopted more sub-grid-scale soil tiling approaches. For example, the CLASS model has the capability of running with either a single soil column or one soil for each surface type but applying grid-box-wide soil properties in these cases (Li and Arora, 2012; Melton and Arora, 2014). Similarly, the NOAH model also assigns a soil column to each surface cover type but imposes identical soil properties for all tiles. The LM3, CABLE and the ORCHIDEE LSMs all assign a soil column to each surface cover type and allow different properties to be assigned to each. In contrast, the E3SM land model (ELM) can represent the soil heterogeneity at different topographic units under a novel topography-based sub-grid structure (Hao et al., 2022).

With this in mind, this paper will describe and evaluate a new flexible surface–soil tiling scheme in JULES, which will allow sub-grid-scale soil heterogeneity to be better represented. The general functionality of the scheme will be described, and a synthetic case study will be used to define and test a range of possible new soil tiling approaches. The changes in model performance will be compared to standard JULES and a high-resolution surrogate "Truth" soil. The aim of this paper is to demonstrate the benefits of soil tiling in JULES by representing the sub-grid-scale soil and surface heterogeneity in the most computationally efficient way.

2 Methodology

2.1 Scheme description

The modular structure and component coupling within JULES has enabled a completely flexible surface–soil interface to be developed. The number of surface tiles in JULES depends on the land configuration being used (see Walters et al., 2019). However, most physical model configurations have nine surface tiles in each grid box, five of which are plant functional types (PFTs) (broadleaf trees, needleleaf trees, C3 (temperate) grass, C4 (tropical) grass and shrubs), and four are non-vegetation types (urban, inland water, bare soil and land ice). Each JULES surface tile calculates its own fluxes of heat, moisture and momentum, derived from bulk aerodynamic formulae through functions of specific humidity, air temperature, wind speed and available energy (see Sect. 2.1 in Best et al., 2011, for more detailed equations). These are averaged and weighted by the fractional cover of each surface tile over the grid box to produce grid box mean components of the surface energy balance.

The flux of water extracted by the vegetation from the soil for transpiration is determined by the root density and the soil moisture availability factor (β). The root density is assumed to follow an exponential distribution with depth, with the depth scale varying between the different PFTs. β is a dimensionless moisture stress factor, which is related to the mean soil moisture concentration in the root zone through the critical and wilting point factors (Eq. 12, Best et al., 2011) and varies between 0 and 1. For soil moisture between saturation and the critical point, no limitation on soil evaporation or plant transpiration is applied (i.e. β equals 1). Below the critical point β decreases linearly from 1 to 0 at the wilting point, whilst below the wilting point no transpiration is possible (i.e. $\beta = 0$). β is also a multiplicative factor in the stomatal conductance equations that are used to calculate photosynthesis (Eq. 11, Best et al., 2011). The soil parameters used here (including the saturated soil water content and critical and wilting points) are calculated from linear equations relating soil moisture to the soil type. The soil types are based on spatially continuous textural properties (sand, silt and clay fractions) and the corresponding soil parameters are calculated using the pedotransfer functions defined by Cosby et al. (1984). The default number of soil layers in JULES is four, with thicknesses 0.1, 0.25, 0.65 and 2.0 m, giving a total soil depth of 3 m. This configuration is designed to correctly capture the variation in soil temperature from sub-daily to annual timescales (Best et al., 2005).

Table 1. Examples of currently used land surface models with their methods for representing sub-grid-scale soil heterogeneity.

Model	Institution	Reference	Soil tiling method
NOAH integrated land model	GFDL	Ek et al. (2003)	Soil per surface type, identical soils
H-TESSEL	ECMWF	Balsamo et al. (2009)	Single dominant soil texture class
CLASS	ECCC	Verseghy (1991, 2000)	Single soil with properties aggregated or soil per surface type
ISBA	Météo-France	Decharme and Douville (2006)	Single soil with properties aggregated
LM3	U.S. Geological Survey	Milly et al. (2014)	Soil per surface type, different soils
ORCHIDEE	IPSL	Ducoudré et al. (1993); de Rosnay (2003)	Soil per surface type, different soils
CABLE	CSIRO/BOM	Kowalczyk et al. (2013)	Soil per surface type, different soils
CLM	NCAR	Oleson et al. (2013)	Single dominant soil
ELM	PNNL	Hao et al. (2022)	Soil per different topographic units, different soils
JULES	Met Office	Best et al. (2011); Clark et al. (2011)	Single dominant soil

Apart from those classified as land ice, a land grid box can be made up of any mixture of surface types. A restriction under the current scheme is that there has to be either 100 % coverage of land ice in a grid box or none because land ice does not have its own prognostic water store. It uses the soil temperature profile to represent the thermal structure of the ice and moisture transport is neglected. As all surface tiles currently share the same soil information for temperature and moisture, this means it is not possible to have a fractional cover of land ice. A new soil tiling scheme could allow a fractional cover of land ice, giving this tile its own soil column and therefore enabling it to represent its own temperature and moisture profile separately from other surface tiles.

The urban surface tile is characterised by a large thermal inertia (one tiled scheme by Best, 2005) and is only in radiative exchange with the underlying soil. Therefore, the capacity of the urban tile to hold water is minimal and drainage of water is preferred over infiltration. This limits the evaporation to periods directly after precipitation, and so the urban tile is therefore equivalent to a dry, one-layer block of concrete with a high heat capacity.

Under the new surface–soil tiling scheme, each grid box has the capability to have a different number of surface tiles and soil tiles and the key feature is managing the connectivity between them. In JULES the surface is implicitly coupled to the atmosphere (Best et al., 2004) and therefore needs to remain fixed at the resolution of the atmospheric driving data. This allows it to capture the fast timescales of the turbulent processes and can sustain longer time steps for computational efficiency. The soil however, responds to slower diffusive processes and hence can be explicitly coupled to the surface without encountering numerical issues. This removes the limitation of the soil needing to be on the same grid as the surface and therefore can be modelled at a higher resolution. As a result of this coupling, each surface tile operates in isolation, interacting with the atmosphere through its own fluxes. Each soil tile also operates in isolation, interacting with the surface tiles above it through the exchange of energy and moisture. There needs to be a precise mapping between the surface and soil tiles to enable them to exchange information between them. This exchange is simple in cases where there is one-to-one mapping between the surface and soil tile. Here evapotranspiration is calculated using the soil moisture availability factor (β) from the soil tile under each surface tile. However, in a grid box where there is a many-to-many interaction between surface and soil tiles, i.e. each surface can access more than one soil column and vice versa, the weighted averages of the β from the soil tiles in each grid box are used by each surface tile to calculate evapotranspiration.

In this work, a synthetic case study has been used to define the surface–soil tile mapping which allowed the representation of a wide range of different surface and soil tile arrangements (shown in Sect. 2.2). Standard JULES currently has nine surface tiles and a single soil column. If each surface tile was then given its own independent soil tile (i.e. by tiling the soil according the surface heterogeneity), then there would be nine surface tiles and nine soil tiles. It is also possible for each surface tile to access multiple soil tiles or to share soil tiles with other surface tiles. In this case the interaction of the surface and subsurface processes can become more complex, but the scheme provides the potential for a computationally optimal configuration with all surface and soil tiles represented.

2.2 Experimental setup

In order to demonstrate the benefits of soil tiling, a range of different surface and soil tile arrangements have been tested

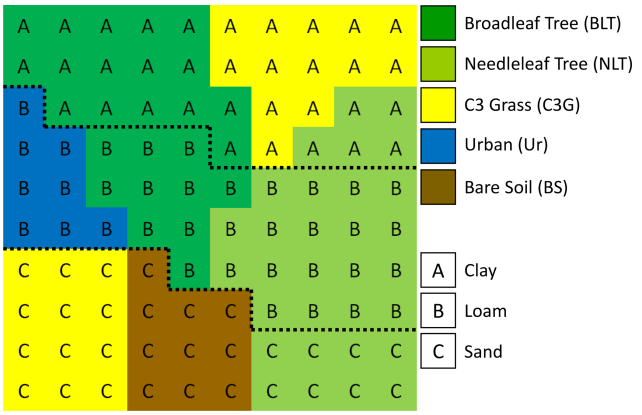

Figure 1. Synthetic grid box used to define and test the new soil tiling configurations. This consists of a 10-by-10-pixel grid, each with one of five different surface types and one of three soil types. The surface types correspond to broadleaf tree (BLT, dark green), needleleaf tree (NLT, light green), C3 grass (C3G, yellow), urban (Ur, blue) and bare soil (BS, brown). The three soil types are clay (A), loam (B) and sand (C) as defined by Cosby et al. (1984).

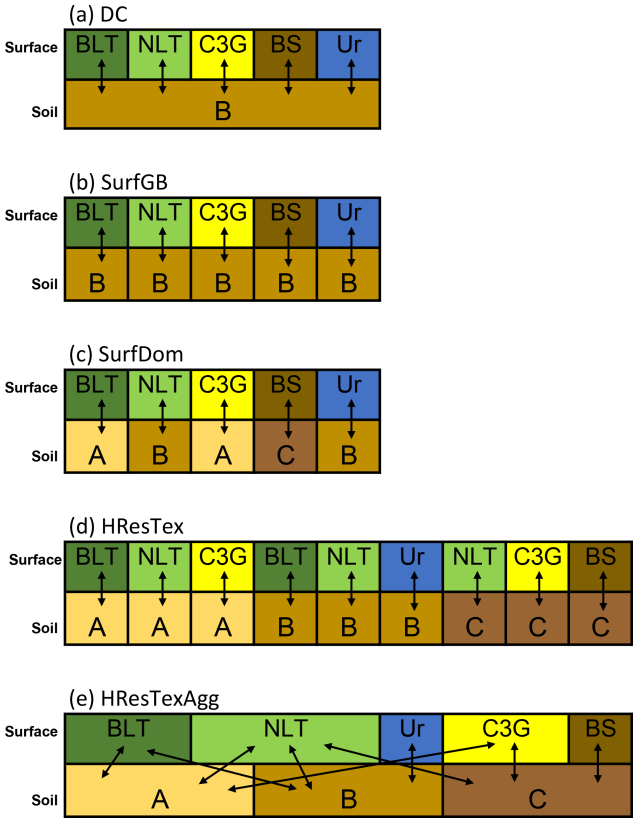

Figure 2. Schematic showing the five surface–soil configurations used in this work (abbreviations as per Fig. 1). **(a)** The "Default Configuration" (DC) currently used by JULES. **(b)** "SurfGB" shows the soil is tiled by surface type with each soil tile having the same grid-box-dominant soil type. **(c)** "SurfDom" shows the soil is tiled by surface type with each soil having the properties of the dominant soil type for that surface. **(d)** "HResTex" uses the higher-resolution soil information to map all the possible combinations of surface and soil tiles. This configuration is considered to be the surrogate truth in the absence of observations. **(e)** "HResTexAgg" is the fully compressed version of the mapping and shows each surface type can interact with multiple soil types and vice versa.

using a synthetic case study and meteorological forcing for a temperate midlatitude site. A single grid box has been generated using an artificial mixture of surface and soil tile combinations (shown by Fig. 1). This was devised in order to represent all five different surface types and a full range of soil textures. The fractions were chosen to give even spread of the different soil–vegetation combinations, allowing a range of different tiling approaches to be simulated and therefore fully testing the capacity of the parameterisation. The artificial grid box represents a resolution of 0.5° with a sub-grid made up of 10 by 10 pixels, each with one of five different surface types and one of three soil types. The surface types correspond to commonly used JULES surface types namely, broadleaf tree (BLT), needleleaf tree (NLT), C3 grass (C3G), urban (Ur) and bare soil (BS) (Best et al., 2011). The three soil types are clay, loam and sand as defined by Cosby et al. (1984). The urban tile is included here because the processes involved here make for a useful and interesting test for the new soil tiling scheme.

In order to apply the mosaic approach to the example in Fig. 1, it would require 100 surface tiles representing each pixel of land cover with a one-to-one mapping to 100 soil tiles with the corresponding soil properties. This can be thought of as a higher-resolution grid for the surface processes compared to the atmospheric forcing, with each surface tile having its own separate soil column. For this study, tiling approaches are being explored which will effectively group the properties of each pixel into a smaller number of discrete categories. This approach is computationally more efficient than the mosaic approach and therefore more appropriate for the modelling systems considered in this work. It is assumed at this stage that there is no interaction between the different soil columns.

The five surface–soil configurations explored in this work are shown in Fig. 2. Figure 2a is the "Default Configuration" (DC) currently used by JULES. Here a single grid box with a dominant loam soil (B, cf. Fig. 1) is shared between all surface tiles. There is a one-to-one mapping between the surface and soil, so each surface type can effectively access all the moisture in that soil. If rainfall infiltrates into the soil via a particular surface tile, there is no constraint for it to be removed by the same surface tile.

Figure 2b and c allow each surface tile to have their own soil tile (i.e. tiling the soil according to the surface type), and this results in five surface types and five soil types. This allows a one-to-one mapping between surface and soil, so each

surface type can effectively access water from one soil column only. In Fig. 2b (SurfGB), the soil is tiled by surface type, but each soil tile has the same grid-box-dominant soil type (B, loam) and therefore has the same properties (as used by DC). This is an appropriate approach if the resolution of the soil data is less than that of the land cover data. In Fig. 2c (SurfDom), the soil is tiled by surface type, but each soil has the properties of the dominant soil type for that surface. Therefore, the soil tiles can be different and are not constrained to the dominant type for the grid box. This approach requires higher-resolution soil information than the previous approach and allows a greater degree of soil heterogeneity within the grid box.

Figure 2d (HResTex) uses the higher-resolution soil information to map all the possible combinations of surface and soil tiles. There are nine combinations of surface and soil in the artificial grid box; hence this requires nine surfaces and nine soils. This is a compressed version of a mosaic approach where the same surface–soil pairs are only calculated once.

Finally, Fig. 2e (HResTexAgg) represents the most computationally efficient method of representing all surface and soil types. Here each surface can interact with all of the soil types as required and vice versa. Therefore, there are only the five surface tiles and three soil tiles. The key difference for this approach is that there is a many-to-many interaction between surface and soil tiles; i.e. each surface can access more than one soil column and the fluxes can be distributed in a more complex way. For example, moisture infiltrating from the BLT surface tile will be distributed between the clay (A, cf. Fig. 1) and the loam (B) soil tiles. This moisture is distributed from the surface to the soil as a proportion of the soil texture; i.e. for BLT, 16/26 goes to clay and 10/26 to loam. Subsequently, soil moisture from the loam soil (B) can be used to supply evapotranspiration for both the BLT and NLT surface tiles.

Each of the five surface–soil configurations has been used to run JULES offline driven using forcing data from WFDEI (WATCH Forcing Data methodology applied to ERA-Interim data, Weedon et al., 2014). The WFDEI data span the period of 1979 to 2012 and are available for all land points at a 0.5 by 0.5° resolution globally at a 3-hourly temporal resolution. Here JULES has been run for an inland location in England (52.25° N, 0.25° E), from 1980 to 2010, using the GL4 science setup (Walters et al., 2014) and a time step of 30 min. Note that this single UK site is not intended to be representative of all climatic regimes. It is used as a demonstration site and results may therefore vary at other locations. Each tiling configuration was allowed to spin up until convergence of soil moisture for the first year of data (i.e. run for multiple years for the first year of data) and then run freely for the whole 30-year period. The output values from these runs have then been compared and evaluated against each other based on their complexity and their ability to represent the "true" heterogeneity of the grid box. Given this is synthetic grid box no observations are available. Therefore, the high-resolution soil run (HResTex) is the closest thing we have to the truth and will be used in the evaluation.

3 Results

In this section, the energy and moisture fluxes from each of the five surface–soil configurations are evaluated against output from the high-resolution soil run (HResTex). This run uses the maximum possible amount of soil information available without using soil tiles and will therefore be used as a surrogate Truth. It is expected that the different soil tiling strategies will result in changes to the surface energy balance and soil moisture due to the way in which energy and water are partitioned between the soils and surfaces. Results will also be compared back to the current single-soil scheme.

3.1 Evaluation of heat and moisture fluxes

The impact of the different soil tiling methods on heat and moisture fluxes is shown in Fig. 3. Plotted here are the 30-year monthly mean surface temperatures, latent and sensible heat fluxes, and total change in soil moisture, averaged over the grid box for each method. The lines for SurfDom and SurfGB are not shown because they overlap with the HResTex run in all variables. The vertical bars represent 1 standard deviation from the DC (solid) line indicating the range in annual variability. All runs remain within 1 standard deviation indicating that the annual averages for all experiments are within the annual variability of the default configuration run.

The impact on average mean surface temperature is much smaller than the basic measure of interannual variability used here. The importance of variations in this quantity is acknowledged, but we note that different users of LSMs will be concerned about different magnitudes and timescales of variation. Therefore, we do not consider surface temperature further. The impact on latent and sensible heat fluxes is much larger especially from May to August. Similarly, the soil moisture change also shows large variations between the methods from April to August as well as additional smaller variations from October through to January. The sensitivity of the fluxes to variations in soil moisture is greatest when the soil is unsaturated. Therefore, from April to August the fluxes are most likely to be impacted by the increased soil moisture limitations on evapotranspiration, which allows more variability. The peak in latent heat flux for the DC (solid line) run is up to $10\,\mathrm{W\,m^{-2}}$ greater than the high-resolution run (HResTex) during June and July (the opposite is the case for the sensible heat flux). The SurfGB and SurfDom experiments (not shown) have a similar annual cycle to HResTex despite the fact that they use far less soil information and tile the soil according to the surface type (as opposed to using high-resolution soils). The reason for this similarity is that they all use a one-to-one mapping between the surface and soil tiles. This results in similar rates of drying, onset of

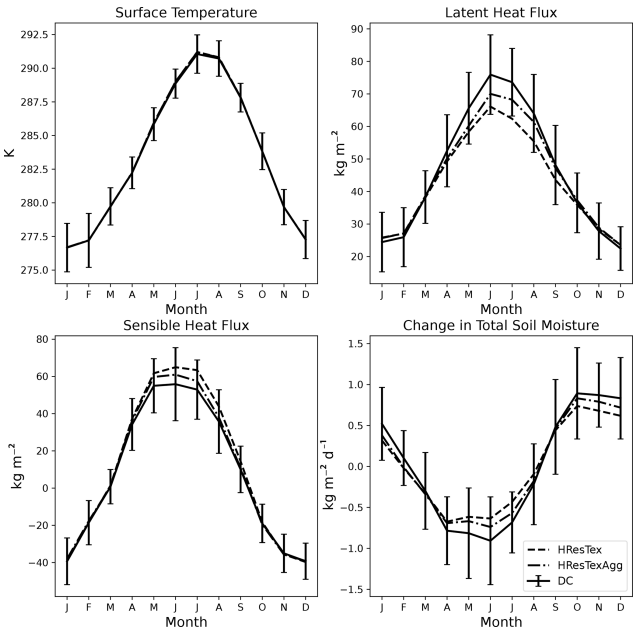

Figure 3. Thirty-year monthly means averaged over the grid box for surface temperature, latent and sensible heat fluxes, and the change in total soil moisture. Thick dashed line: HResTex; dashed–dotted line: HResTexAgg; solid line: DC. Bars are 1 standard deviation from DC line.

soil moisture stress and resultant latent heat fluxes. The more complex HResTexAgg experiment shows a smaller increase in the peak latent heat flux and is much closer in magnitude to the DC experiment, especially in autumn. The change in total soil moisture across all model runs shows a notable dry-down in soil moisture from April to August indicated by the negative change in total soil moisture (see Fig. 3, bottom right plot). For the DC run the dry-down in soil moisture still continues throughout April, May and June. During this time HResTex, SurfGB, SurfDom and HResTexAgg runs have a much slower rate of dry-down and the decrease in soil moisture stays constant. From July onwards the dry-down rate is decreasing across all runs until September when soil moisture increases again in all cases. DC and HResTexAgg then proceed to moisten faster from October onwards. Given that these runs both lost more soil moisture in the summer, they are still slightly drier than HResTex but are gradually becoming less dry over the winter.

3.2 Evaluation of soil moisture availability

Figure 4 shows the mean annual cycle for the soil moisture availability factor (β). Each row in the figure represents the soil layers one to four and each column represents the experiments with decreasing soil heterogeneity from left to right. Each line represents a soil tile with colours representing the surface tiles and line styles representing the soil tile type. For HResTexAgg, there are multiple surface types for each soil type (as per Fig. 2e); hence lines are black and soil tiles are represented by different line styles. As there is only one soil for DC, there is just one line here for each soil layer. The bottom row shows the grid box mean and layer average β for each experiment.

In general Fig. 4 shows that soil tiling is allowing a greater degree of variation in the soil moisture stress through adding more soil tiles and through a dependence of β on the soil type. However, the differences between DC and SurfGB are not due to differences in the soil type (as the soils are the same) but due to the soil tiling on its own. For the DC experiment, the β values for all four soil layers are below 1 and decrease to 0.4 during the summer (0.5 for layer four). When compared to the profiles from SurfGB, SurfDom and HResTex, the soil tiles are allowing β to vary much more. The annual range in β for these experiments is from 0.3 to 1.0 in layer one and 0.2 to 1.0 in layer four. This is because under the soil tiling scheme, the surface tiles have the potential to access soil moisture through roots which are distributed across multiple soil profiles. For SurfGB, SurfDom and HResTex each surface tile will have its own soil profile each with different rooting profiles and water extraction rates associated with them. The resulting grid box mean β for SurfGB is lower than DC; hence on average less soil water is available for these experiments, which can explain the reduction in latent heat flux shown by Fig. 3. For HResTexAgg, each surface tile has access to more than one soil profile and therefore soil moisture can be extracted from more than one rooting profile at once. The average β values are slightly higher than for the other experiments but still lower than DC.

The small differences between SurfDom and SurfGB are due to differences in the soil type only as the number of soil tiles is the same in both runs. SurfDom has BLT and C3G grass with clay soils compared to the loam soils from SurfGB. Clay soils lead to a slightly lower β over all levels and therefore a decrease in the grid box mean β. HResTex also shows that β can be very dependent on the different permutations of surface vegetation and soil types (shown by the spread of the individual curves in Fig. 4). There is a lot of variation occurring between the different levels and between the different surface–soil tile combinations. For example, the β's for BLT clay and BLT sand in layer four differ by up to 0.3 all year round. The differences are very much connected to where the plant roots are (determined through the root densities of the surface tiles) and how available the soil water is for that type of soil and therefore how much extraction can occur. If the surface is a grass tile, then the majority of the roots (greater than 90 %) are in the top 1 m, so water is preferentially extracted from layers one and two. This leads to a larger drop in β during the summer in these layers. If the surface is a tree tile, then the majority of roots are much deeper (83 % of BLTs and 69 % of NLTs have roots in layers three and four) and water is mostly extracted from the deepest two layers of the soil profile. This results in β staying constantly lower throughout the year in layer three and four for all three

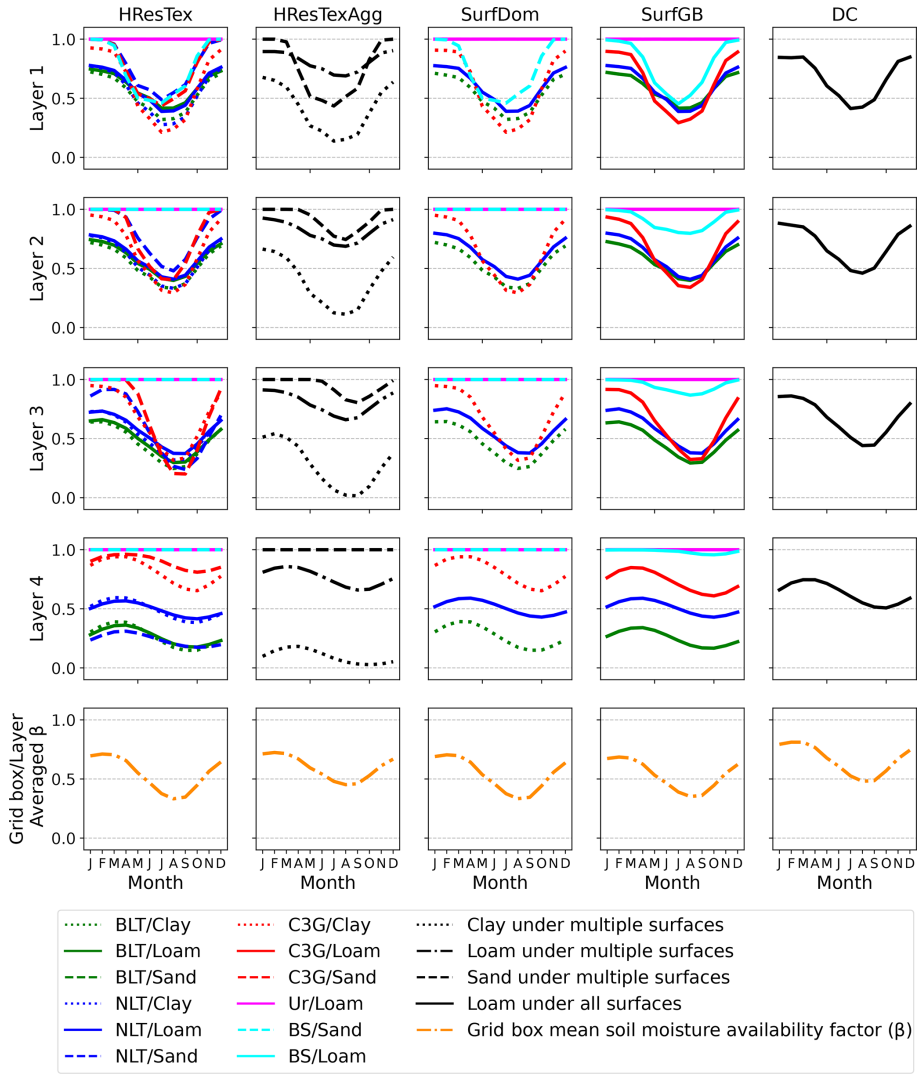

Figure 4. Mean annual cycles for soil moisture availability factor (β). Each row corresponds to a soil model level. Colours represent surface tiles, and line styles represent the soil tile type. For HResTexAgg, there are multiple surface types for each soil type (as per Fig. 2e); hence lines are black and soil tiles are represented by line styles. Final row shows the grid box mean and layered average β.

experiments. If the surface is bare soil, water can only evaporate from the top layer (i.e. the top 10 cm); hence β drops to below 0.5 in layer one over all the experiments. If the soil tile is clay then it will typically hold more water, compared to sandy soils, but this water is held tightly within the pore spaces, leading to lower drainage and higher wilting and critical points; hence soils become water-stressed more easily. In contrast, where the soil tile is a loam then the soil will have considerately higher β and remain closer to the critical point. Differences in the soil type will impact how the soil moisture will drain under gravity and how easily the soil will become stressed.

HResTexAgg has a complex overlap between surface and soil tiles and has very different β characteristics for the individual soils tiles themselves. In particular, the clay soil tile has a much lower β than the other tiles, especially in layer four (up to 0.5 lower). β under the urban tile stays at 1 suggesting that this combination of surface and soil tiles has no impact on the soil moisture.

Despite this huge amount of variation between the surface–soil tile combinations, the grid box mean β for SurfDom and SurfGB show broadly similar patterns implying that adding extra soil information here has made little difference to soil moisture stress and therefore the evaporative fluxes and latent heat flux. However, in general all the soil tiling experiments show the grid box mean β to decrease more during the JJA period compared to the DC experiment.

3.3 Evaluation of grid box mean soil moisture

Figure 5 shows the average annual cycle of grid box mean soil moisture in each layer for the SurfGB and DC experiments. The figure shows that SurfGB tends to have more soil moisture in the summer and less in winter compared to DC. This becomes more emphasised in layer four with the largest differences between the experiments peaking in April and through into October. This result is consistent with the lower latent heat fluxes observed in Fig. 3. The reason these differences in water extraction are occurring is due to the mapping between soil and surface tiles, in particular whether the water in the soil column is shared between surface tiles and how the different soil characteristics are represented through the soil tiling. The DC experiment has a single soil with multiple surface tiles. These surface tiles are able to extract soil moisture from all soil layers at an even rate, with no one soil layer drying out preferentially. Overall this means more soil moisture is lost in total, but the onset of soil moisture stress is slowed, and the dry-down can continue for longer. This leads to a higher peak in latent heat flux shown in Fig. 3. In contrast, SurfGB, SurfDom and HResTex all have a one-to-one mapping between the surface and soil tiles. In each case the surface tile will only be able to access water from the soil column underneath through one rooting profile defined by the surface tile. This results in those tiles with greater root density drying more quickly (than a single soil column), leading to an earlier onset of soil moisture stress compared to the DC experiment. The dry-down is therefore shorter and the peak in latent heat flux is lower. The preferential drying of layers with the highest percentage of roots and largest fraction of surface type has meant that lower values of β have been reached during the summer months compared to the DC experiment. This has started to feed back on the amount of water that is extracted for evapotranspiration, resulting in a slowing of the dry-down and at the same time an increase in soil moisture (show by Fig. 5). Soil tiling is therefore acting in a way to regulate soil moisture loss and therefore evapotranspiration when β is low.

3.4 Evaluation of a more complex tile mappings

HResTexAgg is a more complex case with many-to-many interactions between surface and soil tiles; i.e. each surface can access more than one soil and the soils can have different characteristics. This leads to less preferential drying of layers because there is a more even distribution of roots between the surface types, similar to the DC. The intricacies of the surface–soil mapping in this experiment have led to results that are an intermediate case between the DC and the other experiments. Figure 4 shows very different β characteristics to the other experiments. In particular, the clay soil tile has a much lower β than the other tiles. In contrast, the loam and sand tiles have considerately higher β and remain closer to the critical point. In this case because the surface types are interacting with more than one soil tile, the β values are combined in order to supply the surface tiles with a single soil moisture availability factor. Taking the average β results in a value which is higher than the clay soil tile value but lower than the sand and loam soil tile values. Hence, too much water is extracted from the stressed clay tile and too little from the less stressed sand and loam. This sets up a positive feedback which acts to maintain this difference. Therefore, although the HResTexAgg method does add value over the DC, it does not do as well as SurfDom and SurfGB at reproducing the high-resolution soils experiment, HResTex. It also demonstrates that the non-linear interactions need to be managed correctly in order to gain the benefits of additional soil heterogeneity.

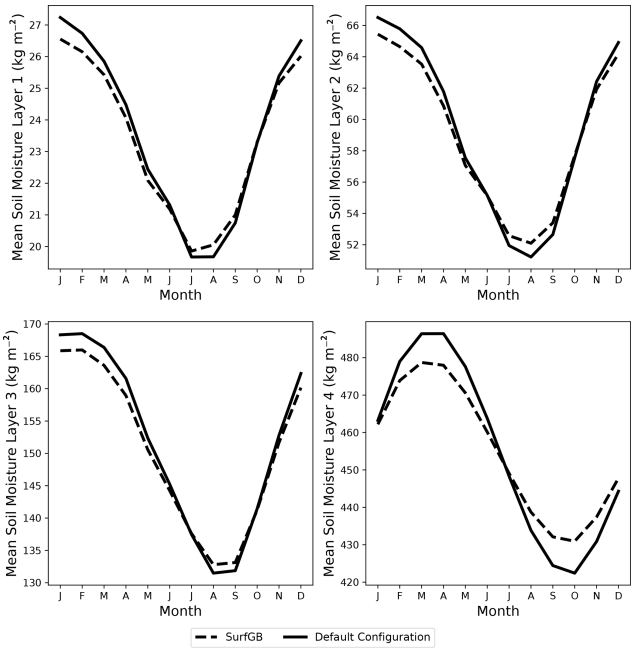

Figure 5. Grid box mean annual cycles of soil moisture in model layers for SurfGB (dashed line) and DC (Default Configuration) (solid line).

4 Conclusions

This paper describes and evaluates a new flexible surface–soil tiling scheme for the land surface model JULES, which allows sub-grid-scale soil heterogeneity to be better represented. The functionality of the scheme has been described and is used to assess potential methods for improving soil heterogeneity.

A synthetic case study has been used to define and test a range of possible new soil tiling methods. Three soil tiling methods have been considered here. Two of these tile the soil by surface type where each surface has its own soil tile (using either the grid-box-dominant, SurfGB, or the surface-

tile-dominant soil, SurfDom). A third method is a many-to-many approach (HResTexAgg) whereby the surface can interact with all of the soil types as required and vice versa. The changes in model performance have been compared to the single shared soil scheme currently used by JULES (DC) and a high-resolution surrogate Truth soil (HResTex), which uses higher-resolution soil property data to map all possible combinations of surface and soil tiles.

Overall, soil tiling introduces a decrease in monthly mean latent heat flux (increase in sensible heat flux) compared to the standard DC run, with the largest differences observed from May to August. Soil tiling methods that tile the soil according to the surface type (SurfGB and SurfDom) have almost identical fluxes to HResTex. The annual cycle of the change in total soil moisture shows a notable dry-down from April to August. The SurfGB, SurfDom and HResTex runs are comparable and show a much slower rate of dry-down compare to the DC run. These runs also show a much greater degree of variation in soil moisture stress compared to the DC run.

The variations between the experiments are due to differences in the amount of water that the vegetation is able to extract through the roots from soil moisture, and this is dependent on the type of soil and the distribution of roots in the soil (which depend on the surface type). The DC experiment has a single soil with multiple surface tiles. These surface tiles are able to extract soil moisture from all soil layers at a more even rate, with no one soil layer drying out preferentially. Hence, the onset of soil moisture stress is slowed, and the dry-down can continue for longer, leading to a higher peak in latent heat flux and more soil moisture lost in total. In contrast, SurfGB, SurfDom and HResTex all have a one-to-one mapping between the surface and soil tiles. The surface type will only be able to access water from the soil column underneath through one rooting profile defined by the surface type. This results in certain layers with greater root density drying more quickly, leading to an earlier onset of soil moisture stress compared to the DC experiment. The dry-down is therefore shorter and the peak in latent heat flux is lower. These differences in water extraction rates have led to the large variation in β across the soil tiles. The preferential drying of layers with the highest percentage of roots and largest fraction of surface type has meant that lower values of β have been reached during the summer months compared to the DC experiment. This feeds back to the amount of water that is extracted for evapotranspiration, resulting in a slowing of the dry-down and at the same time an increase in soil moisture. Soil tiling is therefore acting to regulate grid box mean soil moisture loss and evapotranspiration when β is low.

The more complicated, aggregated approach (HResTexAgg) requires more soil information and has complex interactions between the soil and surface tiles, but the reduction in latent heat flux is less. For this case, the extraction of water from the soil tiles does not yield the correct transpiration due to the non-linear combinations of the soil moisture stress for vegetation from each soil type. This results in too much water being extracted from some soils and too little from others.

Despite the increase in heterogeneity between SurfGB, SurfDom and HResTex, the results from these experiments are very similar suggesting that it is the changes to the way vegetation accesses the soil moisture that is more important rather than the variability added by the soil heterogeneity itself (although this is still a factor). This demonstrates that any of these three methods would be appropriate to represent sub-grid-scale soil heterogeneity in JULES. However, tiling according to the surface type and using the dominant soil for that surface type (SurfDom), gives the best compromise between giving the biggest positive impact without requiring very high-resolution soil information (like HResTex). It still allows some heterogeneity between soil tiles (unlike SurfGB), which is important for other hydrological soil processes (such as lateral flow) and is the closest to the high-resolution Truth. Overall this method provides the most flexibility and is the most computationally efficient way to introduce sub-grid-scale soil heterogeneity into JULES.

5 Scheme applications and future work

There are many applications which will be improved by the addition of this scheme. For example, Smith et al. (2022) demonstrate the importance of soil tiling for simulating discontinuous permafrost and use a simplified form of the code to address biases in methane emissions. This study also uses lateral soil moisture flow to improve the snow depth, soil moisture and temperature over the permafrost landscape. Another application is the recent implementation of the lake model, FLake (Rooney and Jones, 2010), into standalone JULES. It has had issues with correctly diagnosing the soil temperatures underneath the lakes. Soil tiling by surface type would allow lake tile soils to be thermally coupled in a different way to standard soil–atmosphere coupling, such that soil temperatures could be adjusted to deal with depth. The new scheme will also provide the opportunity to introduce a fractional cover of land ice. Under the existing setup there has to be either 100 % coverage of land ice in a grid box or none because land ice does not have its own prognostic water store. The new scheme could give the land ice tile its own soil column and therefore enable it to represent its own temperature and moisture profile separately from other surface tiles.

Given a synthetic example case study is used in this work, it cannot be evaluated against observations. In order for observations to be used, suitable-resolution observation data are required. However, area-representative observations of soil moisture and surface fluxes (latent and sensible heat flux) are challenging to measure at the grid scales of interest here. Many measurements of soil moisture and surface fluxes are at a single point, which may not be representative of the surrounding area. Soil moisture is spatially heterogeneous,

whilst the surface fluxes are dependent on the footprint area. On the other hand, observations of soil moisture using satellite microwave sensing can provide integrated values of near-surface soil moisture at resolutions of hundreds to thousands of square kilometres, but they are unable to penetrate more than a few centimetres into the soil (and therefore do not represent root zone soil moisture) and the signal can be masked by snow or dense vegetation. Given this lack of suitable observations, a high-resolution (atmosphere, surface and soil) simulation could be used as surrogate observations in future work.

Additionally, only one climate is tested here (midlatitude temperate). It is possible that the conclusions of this study could change under different climates. For example, the energy and water fluxes at an arid site are likely to be less sensitive to variations in soil moisture and therefore soil heterogeneity would be less important. However, the context of this work focused on testing the schemes limits and capabilities using an artificial grid box and therefore the impact of using other climates will be considered for future work.

Finally, the work in this paper has not yet considered the impact of lateral flow of soil moisture between soil columns, which will become more significant as resolution is increased. By allowing lateral flow, the soil profiles within a grid box could exchange water through slope and diffusive processes, thus representing hydrological variability in a more realistic way. This could impact the accuracy of the surface fluxes at sufficiently high resolution and may have wider significance when used within a coupled weather and climate model. Hence, it is possible that the inclusion of lateral flows could influence the conclusions of this study and should be considered for future experiments.

Code and data availability. The JULES model code is freely available to anyone for non-commercial use from the Met Office Science Repository Service (MOSRS) (https://code.metoffice.gov.uk/, last access: 3 August 2022). Registration is required and is subject to completion of a software licence (for details of licensing, see https://jules.jchmr.org/content/code, last access: 3 August 2022). Visit the registration page (http://jules-lsm.github.io/access_req/JULES_access.html, last access: 3 August 2022) to request code access and a MOSRS account. The results presented in this paper were obtained by running JULES from the following branch: https://code.metoffice.gov.uk/trac/jules/browser/main/branches/dev/heatherashton/vn3.4.1_soil_tiling?rev=23611 (last access: 14 February 2023). This is a development branch of JULES version 3.4.1 which includes the new surface–soil tiling scheme. This branch can be accessed and downloaded from the Met Office Science Repository Service once the user has registered for an account, as outlined above. The input and output data and plotting scripts used in this paper are provided at https://doi.org/10.5281/zenodo.6954142 (Rumbold et al., 2022). The experiments described in this paper use the configurations prescribed in the following branch: https://code.metoffice.gov.uk/trac/jules/browser/main/branches/dev/heatherashton/vn3.4.1_soil_tiling/configurations?rev=23611 (last access: 14 February 2023). The "Gzipped" WFDEI files are freely available from the WATCH ftp site at IIASA, Vienna (online: ftp://rfdata:forceDATA@ftp.iiasa.ac.at (Weedon et al., 2014); click on /WATCH_Forcing_Data and then /WFDEI, or use the following for ftp downloads: site – ftp.iiasa.ac.at; username – rfdata; password – forceDATA; then use cwd/WFDEI). The /WFDEI directory includes files listing grid box elevations and locations. An alternative source of WFDEI data is provided by the DATAGURU website for climate-related data at Lund University (http://dataguru.nateko.lu.se/, last access: 14 February 2023; log in, then go to "Application"). More information is available from Weedon et al. (2014) in Sect. 6, pp. 8 and 9. The script available at https://doi.org/10.5281/zenodo.6954142 (Rumbold et al., 2022) extracts the WFDEI data for the single latitude–longitude point used in this paper.

Author contributions. MJB initiated the research into implementing a sub-grid-scale soil heterogeneity scheme within JULES and provided general scientific guidance throughout the paper. RJJG and HSR determined the scope of the code and wrote it, while RJJG set up and ran the experiments. HSR did the analysis and wrote the paper.

Competing interests. The contact author has declared that none of the authors has any competing interests.

Disclaimer. Publisher's note: Copernicus Publications remains neutral with regard to jurisdictional claims in published maps and institutional affiliations.

Acknowledgements. The authors thank the reviewers and editor for their comments and suggestions. The authors also thank Adrian Lock for helpful comments on preparing this paper.

Financial support. This research has been supported by the Joint Business, Energy and Industrial Strategy, UK Government, and the Defra Met Office Hadley Centre Climate Programme (GA01101).

Review statement. This paper was edited by Christian Folberth and reviewed by two anonymous referees.

References

Balsamo, G., Viterbo, P., Beljaars, A., Hurk, B. V. D., Hirschi, M., Betts, A. K., and Scipal, K.: A Revised Hydrology for the ECMWF Model: Verification from Field Site to Terrestrial Water Storage and Impact in the Integrated Forecast System, J. Hydrometeorol., 10, 623–643, 2009.

Best, M.: Representing urban areas within operational numerical weather prediction models, Bound.-Lay. Meteorol., 114, 91–109, https://doi.org/10.1007/s10546-004-4834-5, 2005.

Best, M., Beljaars, A., Polcher, J., and Viterbo, P.: A proposed structure for coupling tiled surfaces with the planetary boundary layer, J. Hydrometeorol., 5, 1271–1278, 2004.

Best, M. J., Cox, P. M., and Warrilow, D.: Determining the optimal soil temperature scheme for atmospheric modelling applications, Bound.-Lay. Meteorol., 114, 111–142, 2005.

Best, M. J., Pryor, M., Clark, D. B., Rooney, G. G., Essery, R. L. H., Ménard, C. B., Edwards, J. M., Hendry, M. A., Porson, A., Gedney, N., Mercado, L. M., Sitch, S., Blyth, E., Boucher, O., Cox, P. M., Grimmond, C. S. B., and Harding, R. J.: The Joint UK Land Environment Simulator (JULES), model description – Part 1: Energy and water fluxes, Geosci. Model Dev., 4, 677–699, https://doi.org/10.5194/gmd-4-677-2011, 2011.

Betts, A. K. and Ball, J. H.: FIFE surface climate and site-average dataset 1987–89, J. Atmos. Sci., 55, 1091–1108, 1998.

Clark, D. B., Mercado, L. M., Sitch, S., Jones, C. D., Gedney, N., Best, M. J., Pryor, M., Rooney, G. G., Essery, R. L. H., Blyth, E., Boucher, O., Harding, R. J., Huntingford, C., and Cox, P. M.: The Joint UK Land Environment Simulator (JULES), model description – Part 2: Carbon fluxes and vegetation dynamics, Geosci. Model Dev., 4, 701–722, https://doi.org/10.5194/gmd-4-701-2011, 2011.

Cosby, B., Hornberger, G., Clapp, R., and Ginn, T.: A statistical exploration of the relationships of soil moisture characteristics to the physical properties of soils, Water Resour. Res., 20, 682–690, https://doi.org/10.1029/WR020i006p00682, 1984.

Decharme, B. and Douville, H.: Introduction of a sub-grid hydrology in the ISBA land surface model, Clim. Dynam., 26, 65–78, 2006.

de Rosnay, P.: A GCM Experiment on Time Sampling for Remote Sensing of Near-Surface Soil Moisture, J. Hydrometeorol., 4, 448–459, 2003.

Ducoudré, N., Laval, K., and Perrier, A.: SECHIBA, a New Set of Parameterizations of the Hydrologic Exchanges at the Land-Atmosphere Interface within the LMD Atmospheric General Circulation Model, J. Climate, 6, 248–273, 1993.

Ek, M. B., Mitchell, K. E., Lin, Y., Rogers, E., Grunmann, P., Koren, V., Gayno, G., and Tarpley, J. D.: Implememtation of Noah land surface model advances in the National Centers for Environmental Prediction operational mesoscale Eta model, J. Geophys. Res., 108, 163–166, 2003.

Eltahir, E. A.: A soil moisture – rainfall feedback mechanism 1. Theory and observations, Water Resour. Res., 34, 765–776, 1998.

Eltahir, E. A. and Bras, R. L.: Precipitation recycling, Rev. Geophys., 34, 367–378, 1996.

Essery, R. L. H., Best, M. J., Betts, R. A., Cox, P. M., and Taylor, C. M.: Explicit Representation of Subgrid Heterogeneity in a GCM Land Surface Scheme, J. Hydrometeorol., 4, 530–543, 2003.

Hao, D., Bisht, G., Huang, M., Ma, P.-L., Tesfa, T., Lee, W.-L., Gu, Y., and Leung, L. R.: Impacts of Sub-Grid Topographic Representations on Surface Energy Balance and Boundary Conditions in the E3SM Land Model: A Case Study in Sierra Nevada, J. Adv. Model. Earth Sy., 14, e2021MS002862, https://doi.org/10.1029/2021MS002862, 2022.

Heinemann, G. and Kerschgens, M.: Comparison of methods for area-averaging surface energy fluxes over heterogeneous land surfaces using high-resolution non-hydrostatic simulations, Int. J. Climatol., 25, 379–4032, 2005.

Hohenegger, C., Brockhaus, P., Bretherton, C., and Schär, C.: The soil moisture-precipitation feedback in simulations with explicit and parameterized convection, J. Climate, 22, 5003–5020, 2009.

Kowalczyk, E., Stevens, L., Law, R., Dix, M., Wang, Y., Harman, I., Haynes, K., Srbinovsky, J., Pak, B., and Ziehn, T.: The land surface model component of ACCESS: description and impact on the simulated surface climatology, Aust. Meteorol. Ocean., 63, 65–82, 2013.

Li, R. and Arora, V. K.: Effect of mosaic representation of vegetation in land surface schemes on simulated energy and carbon balances, Biogeosciences, 9, 593–605, https://doi.org/10.5194/bg-9-593-2012, 2012.

Melton, J. R. and Arora, V. K.: Sub-grid scale representation of vegetation in global land surface schemes: implications for estimation of the terrestrial carbon sink, Biogeosciences, 11, 1021–1036, https://doi.org/10.5194/bg-11-1021-2014, 2014.

Milly, P. C. D., Malyshev, S. L., Shevliakova, E., Dunne, K. A., Findell, K. L., Gleeson, T., Liang, Z., Phillipps, P., Stouffer, R. J., and Swenson, S.: An Enhanced Model of Land Water and Energy for Global Hydrologic and Earth System Studies, J. Hydrometeorol., 15, 1739–1761, 2014.

Noilhan, J. and Mahfouf, J.: The ISBA land surface parametrization scheme, Global Planet. Change, 13, 145–159, 1999.

Oleson, K., Lawrence, D., Bonan, G., Drewniak, B., Huang, M., Koven, C., Levis, S., Li, F., Riley, W., Subin, Z., Swenson, S., Thornton, P., Bozbiyik, A., Fisher, R., Heald, C., Kluzek, E., Lamarque, J.-F., Lawrence, P., Leung, L., Lipscomb, W., Muszala, S., Ricciuto, D., Sacks, W., Sun, Y., Tang, J., and Yang, Z.-L.: Technical description of version 4.5 of the Community Land Model (CLM), No. NCAR/TN−503+STR), https://doi.org/10.5065/D6RR1W7M, 2013.

Rooney, G. G. and Jones, I. D.: Coupling the 1D lake model Flake to the community land surface model JULES, Boreal Env. Res., 15, 501–512, 2010.

Rumbold, H., Gilham, R., and Best, M. Assessing methods for representing soil heterogeneity through a flexible approach within the Joint UK Land Environment Simulator (JULES) at version 3.4.1, Zenodo [data set and code], https://doi.org/10.5281/zenodo.6954142, 2022.

Smith, N. D., Burke, E. J., Schanke Aas, K., Althuizen, I. H. J., Boike, J., Christiansen, C. T., Etzelmüller, B., Friborg, T., Lee, H., Rumbold, H., Turton, R. H., Westermann, S., and Chadburn, S. E.: Explicitly modelling microtopography in permafrost landscapes in a land surface model (JULES vn5.4_microtopography), Geosci. Model Dev., 15, 3603–3639, https://doi.org/10.5194/gmd-15-3603-2022, 2022.

Verseghy, D. L.: CLASS: A Canadian Land Surface Scheme for GCMS. I. Soil Model, Int. J. Climatol., 11, 111–133, 1991.

Verseghy, D. L.: The Canadian land surface scheme (CLASS): Its history and future, Atmos. Ocean, 38, 1–13, https://doi.org/10.1080/07055900.2000.9649637, 2000.

Walters, D., Baran, A. J., Boutle, I., Brooks, M., Earnshaw, P., Edwards, J., Furtado, K., Hill, P., Lock, A., Manners, J., Morcrette, C., Mulcahy, J., Sanchez, C., Smith, C., Stratton, R., Tennant, W., Tomassini, L., Van Weverberg, K., Vosper, S., Willett, M.,

Browse, J., Bushell, A., Carslaw, K., Dalvi, M., Essery, R., Gedney, N., Hardiman, S., Johnson, B., Johnson, C., Jones, A., Jones, C., Mann, G., Milton, S., Rumbold, H., Sellar, A., Ujiie, M., Whitall, M., Williams, K., and Zerroukat, M.: The Met Office Unified Model Global Atmosphere 7.0/7.1 and JULES Global Land 7.0 configurations, Geosci. Model Dev., 12, 1909–1963, https://doi.org/10.5194/gmd-12-1909-2019, 2019.

Walters, D. N., Williams, K. D., Boutle, I. A., Bushell, A. C., Edwards, J. M., Field, P. R., Lock, A. P., Morcrette, C. J., Stratton, R. A., Wilkinson, J. M., Willett, M. R., Bellouin, N., Bodas-Salcedo, A., Brooks, M. E., Copsey, D., Earnshaw, P. D., Hardiman, S. C., Harris, C. M., Levine, R. C., MacLachlan, C., Manners, J. C., Martin, G. M., Milton, S. F., Palmer, M. D., Roberts, M. J., Rodríguez, J. M., Tennant, W. J., and Vidale, P. L.: The Met Office Unified Model Global Atmosphere 4.0 and JULES Global Land 4.0 configurations, Geosci. Model Dev., 7, 361–386, https://doi.org/10.5194/gmd-7-361-2014, 2014.

Weedon, G. P., Balsamo, G., Bellouin, N., Gomes, S., Best, M. J., and Viterbo, P.: The WFDEI meteorological forcing dataset: WATCH Forcing Data methodology applied to ERA-Interim reanalysis data, Water Resour. Res., 50, 7505–7514, https://doi.org/10.1002/2014WR015638, 2014 (data available at: ftp://rfdata:forceDATA@ftp.iiasa.ac.at, last access: 14 Febuary 2023).